Sampled-Data Cooperative Adaptive Cruise Control of Vehicles With Sensor Failures

Ge Guo, *Member, IEEE*, and Wei Yue

***Abstract*—This paper investigates sampled-data cooperative adaptive cruise control (CACC) of vehicles with sensor failures. A novel switched sampled-data CACC system model is established, in which the effect of sensor failure is involved. Based on the new model, a design method of state feedback controllers that can robustly stabilize the CACC system is presented via the switched system approach. The obtained controller is complemented by additional conditions that are established for guaranteeing string stability and zero steady-state velocity error, which yields a useful string stable CACC algorithm. Several quantitative relations of parameters, including the sensor complete-failure rate, the system decay rate, and sampling period, are also derived. The effectiveness and advantage of the presented methodology are demonstrated by both numerical simulations and experiments with laboratory-scale Arduino cars.**

***Index Terms*—Cooperative adaptive cruise control (CACC), exponential stability, sampled-data control, sensor failure, string stability.**

I. Introduction

TRAFFIC congestion has become a serious problem in most big cities. In China alone, traffic congestion and environmental pollution are costing billions of dollars each year with hundreds of thousands of people killed or injured. In the past decades, considerable efforts have been devoted to automated highway/vehicle systems, aiming at finding new technologies for reducing road congestion and improving traffic efficiency. In various recent research works, cooperative adaptive cruise control (CACC) has been regarded as one of the most promising techniques in intelligent transportation system applications [1]–[3]. CACC is an extension of the existing longitudinal control function known as adaptive cruise control (ACC), which relieves the driver from adjusting the speed to the vehicle in front. When one car is following another in the ACC mode, amplifications in acceleration may occur due to delays in sensing the behavior of the preceding vehicle and actuating the own vehicle. If there is a third following vehicle, it will experience an even stronger amplification of the acceleration. The longer the queue of vehicles, the stronger the required accelerations (or decelerations), creating shock waves throughout the string of vehicles [4], [5]. CACC can be seen as a smarter ACC in which vehicle control does not rely solely on onboard sensors (such as radar); instead, radio communication is introduced to exchange information between vehicles. The use of wireless communication allows vehicles to adapt to those ahead and, hence, mitigate the shock wave effect. A group of vehicles coordinating via CACC is referred to as a platoon. In addition to lowered energy consumption due to smoother traffic, it has been shown that reductions in fuel consumption due to reduced aerodynamic drag can also be achieved when vehicles travel closer together in a platoon [6], [7]. The synthesis of a CACC system consists in designing a spacing policy and a controller to regulate the speed of the vehicle [1]. Generally, there are two types of spacing policies that are widely used for vehicular cooperative control, i.e., the constant-spacing policy and the constant-time-headway-spacing policy, depending on whether the required spacing of the vehicle is dependent on its speed. The constant-time-headway-spacing policy applies mainly to ACC of a single car following another one, which has been equipped in many passenger cars [8]. The constant-spacing policy is widely used for platoon control of a string of vehicles. Here, as in [3], we will investigate a combined spacing policy.

Since adjacent vehicles in a CACC system are dynamically coupled, sudden changes in the velocity of a preceding vehicle may affect those behind or even amplify as they propagate along the string of vehicles. Such a phenomenon is known as the *slinky effect*, which may not only make the string of vehicles unstable but also yield poor ride quality and, in extreme cases, even result in rear-ending accidents to upstream vehicles. To date, significant research attention has been contributed to this topic in different aspects and from different viewpoints. To name just a few, Lidstrom *et al.* [9] investigated a modular CACC system that can switch between ACC and CACC modes to improve safety during decelerations, Guvenç *et al.* [10] introduced a successful CACC implementation with Team Mekar cars in the Grand Cooperative Driving Challenge project, Naus *et al.* [11] studied practical string stability of a CACC system with the constant-time-headway-spacing policy considering the limitation of the communication link, Middleton and Braslavsky [12] investigated the effect of limited communication range on string stability, and Xiao and Gao [13] addressed the fuel and brake delays and lags and gave a sliding-mode controller that guarantees string stability. Other closely related papers on CACC include [14]–[16]. To be specific, van Arem *et al.* [14] studied the impact of CACC on traffic flow;

Manuscript received May 13, 2013; revised September 9, 2013, January 7, 2014, and March 21, 2014; accepted March 29, 2014. Date of publication May 13, 2014; date of current version December 1, 2014. This work was supported in part by the National Natural Science Foundation of China under Grants 61273107, 61304192, and 61174060; by the Dalian Leading Talent Project under Grant 2012Z0036; by the Fundamental Research Funds for the Central Universities under Grants 852004 and 3132013334; and by the Shenzhen Knowledge Innovation Plan Project under Grant JCYJ20130401172046453. The Associate Editor for this paper was H. Jula.

The authors are with the School of Control Science and Engineering, Dalian University of Technology, Dalian 116023, China (e-mail: geguo@yeah.net; yuewei811010@163.com).

Color versions of one or more of the figures in this paper are available online at http://ieeexplore.ieee.org.

Digital Object Identifier 10.1109/TITS.2014.2316016

Lei *et al.* [15] considered the impact of date rate and packet loss on string stability of CACC systems, giving tight bounds on beacon-sending frequency and packet loss ratio; and Desjardins and Chaib-Draa [16] investigated CACC with delays in the sensing and communication units.

It is worth mentioning that most of the existing results on CACC generally assume that the measurements of the onboard sensors are reliable all the time. However, contingent failures might happen to sensors in practical cars for reasons such as poor visibility due to rain or sandstorm, low battery power, and interference of radar signals (see, e.g., [17]). Different factors may cause different failure properties. For example, when a car is running in the rain, the signal-to-noise ratio of a radar sensor may noticeably decay with the rainfall intensity, and the failure rate may increase with the rain level until momentary freezing or complete failure happens [18], [19]. Vulnerability of automobile radar/lidar sensors to weather phenomena such as rain and snow (which is due to the scattering of radio waves from particulate matters such as raindrops or snowflakes) was studied by many researchers in [17]–[19]. In addition to adverse weather phenomena, rapid and continuous background changing may also yield inaccurate measurement (of position, velocity, and acceleration) [20]. Under such situations, the vehicle can still have access to the state (e.g., acceleration) of the preceding car via the wireless network but might be unaware of the intervehicle distance measured by onboard sensors, which may imperil the string stability of the queue of vehicles. This issue was investigated in [21] in an ACC setting, where for a string of vehicles running along designated highway segments with heavy traffic and scarce visibility, a decentralized communication and monitoring system was developed to assist drivers visually and acoustically. However, the driving assistant technology suggested is not applicable to the fully automated CACC system that we are interested in here. How would sensor failures affect the cooperative control of a string of vehicles still remains an open and challenging problem, and this is the intention of this paper.

As a CACC system is a standard digital control system, here, we are interested in the design and implementation of CACC systems in a sampled-data control context. This is not just because a CACC system is a standard digital control system, the motivation comes from a hidden phenomenon observed in a series of experiments with Arduino cars [22]. It is noticed in the experiments that, although a smaller sampling period leads to a better stability performance, it is often accompanied by more zero data (namely, complete failures) read from the onboard infrared sensors GP2D12 (produced by Sharp Corporation and has an integrated function of signal processing and analog voltage output [23]) in a given period of time. The relationship between the sampling period and the rate in which the sensor completely fails is shown in Fig. 1. This phenomenon makes the problem of vehicle cooperative control under sensor failures further complicated.

The aim of this paper is to set up a CACC framework that takes full consideration of the sensor failure phenomenon and the effect of the sampling period on sensor failure. We first model the CACC system in the context of a switched sampled-data system, which is then equivalently written as a continuous-time switched delay system by using model transformation. Based on the average dwell time technique and the Lyapunov method, sufficient conditions for the existence of output feedback controllers are derived, which ensure the exponential stability of the CACC system. Based on these conditions, some specific quantitative relations between the system decay rate, the sampling period, and the sensor complete-failure rate are derived. With these relations, not only the individual vehicle stability and string stability can be guaranteed with a desired exponential decay rate but also zero steady-state velocity errors can be achieved. As will be shown later in both numerical simulations and experiments with Arduino cars, the presented method can serve as an effective algorithm for practical use.

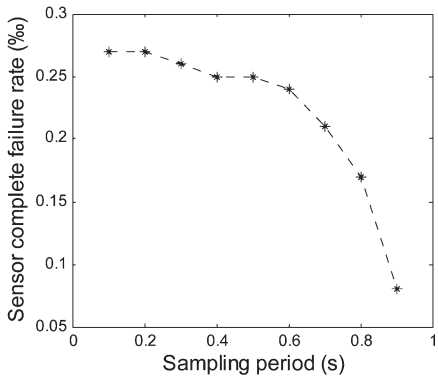

Fig. 1. Relationship between the sampling period and the sensor complete-failure rate (infrared sensor GP2D12, Sharp Corporation).

The rest of this paper is organized as follows. In Section II, after a brief description of the dynamics of the vehicle model, a switched CACC model is established with sensor failures taken into consideration. In Section III, a switched controller design procedure is suggested for dealing with sensor failures and preceding vehicle disturbance. In Section IV, sufficient conditions for the controller to achieve string stability and zero steady-state velocity errors are presented to complement the switched controller, leading to a string stable CACC algorithm. Simulations and experiments are presented in Section V, showing the usefulness and advantage of the proposed methods. The conclusions are given in Section VI.

Notation: In this paper, $\lambda_{\max}(\cdot)$ and $\lambda_{\min}(\cdot)$ are the maximal and minimal eigenvalues of a matrix, respectively. The superscript "T" stands for matrix transposition, R^n denotes the n-dimensional Euclidean space, and the notation $P > 0 (\geq 0)$ means that matrix P is real symmetric and positive definite (semidefinite). In symmetric block matrices, we use an asterisk $(*)$ to represent a term that is induced by symmetry, and $\mathrm{diag}\{\cdot\}$ stands for a block-diagonal matrix. Matrices, if their dimensions are not explicitly stated, are assumed to be compatible for algebraic operations.

II. Problem Formulation

Consider a CACC system composed by n vehicles (see Fig. 2) running in a horizontal environment. Each vehicle transmits its acceleration to its follower via a wireless communication channel. All followers are equipped with onboard sensors to measure the distance and relative velocity between

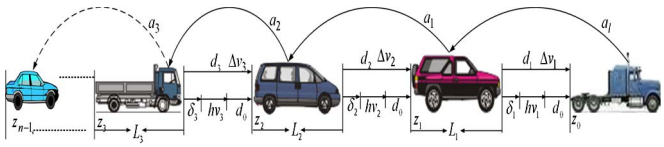

Fig. 2. CACC system.

it and its preceding vehicle. In what follows, we will describe in detail the CACC vehicle model, the sensor failure effect, and our objective one by one.

A. CACC System Modeling

Denote by z_i, v_i, and a_i the ith $(i = 0, \ldots, n-1)$ vehicle's position, velocity, and acceleration, with $i = 0$ standing for the lead vehicle and the others being followers. Define the spacing error of the ith following vehicle as

$$\delta_i = z_{i-1} - z_i - L_i - hv_i - d_0 (z_0 = 0 \text{ in } \delta_1) \tag{1}$$

where h is the time gap, d_0 is a given minimum distance, and L_i is the length of the vehicle. Then, the dynamics of the ith following vehicle can be modeled by the following nonlinear differential equations (see, e.g., [24]–[26] for details):

$$\begin{aligned} \dot{\delta}_i &= v_{i-1} - v_i - h\dot{v}_i \\ \Delta\dot{v}_i &= a_{i-1} - a_i \\ \dot{a}_i &= f_i(v_i, a_i) + g_i(v_i)c_i \end{aligned} \tag{2}$$

where c_i is the control input of the ith vehicle's engine/brake, with $c_i \geq 0$ and $c_i < 0$ representing the throttle input and the brake input, respectively, and $f_i(v_i, a_i)$ and $g_i(v_i)$ are given by

$$\begin{aligned} f_i(v_i, a_i) &= -\frac{1}{\varsigma_i}\left(\dot{v}_i + \frac{\sigma A_i c_{di}}{2m_i} v_i^2 + \frac{d_{mi}}{m_i}\right) - \frac{\sigma A_i c_{di} v_i a_i}{m_i} \\ g_i(v_i) &= \frac{1}{\varsigma_i m_i} \end{aligned}$$

where σ is the specific mass of the air, m_i is the vehicle mass, A_i is the cross-sectional area, $\sigma A_i c_{di}/2m_i$ is the air resistance, c_{di} is the drag coefficient, d_{mi} is the mechanical drag, and ς_i is the engine time constant.

Notice that this is not the first time the spacing policy in the form of (1) is used; it was previously introduced in [3]. The difference lies in that parameter h in this paper is a constant that is given, whereas in [3], it is not a constant but a function to be designed. Specifically, it is designed in [3] as a nonlinear function of vehicle speed.

We adopt the following control law:

$$c_i = u_i m_i + \sigma A_i c_{di} v_i^2/2 + d_{mi} + \varsigma_i \sigma A_i c_{di} v_i a_i \tag{3}$$

where u_i is the additional input signal to be designed so that the closed-loop system can satisfy certain performance criteria. Obviously, this control law achieves feedback linearization, since, after introducing (3), the third equation in (2) becomes

$$\dot{a}_i(t) = -a_i(t)/\varsigma_i + u_i(t)/\varsigma_i. \tag{4}$$

Note that with the controller in (3), we can achieve two objectives: 1) linearization of the ith vehicle dynamics; and 2) simplification of the system model by excluding from the vehicle dynamics some characteristic parameters (e.g., the mechanical drag, the mass, and the air resistance).

By combining the dynamics of the vehicle (4) and (1) and setting $a_{i-1}(t) = w_i(t)$, which is transmitted from the preceding vehicle with a communication delay τ_i, we end up with the following state space equation for the CACC system:

$$\dot{x}_i(t) = A_i x_i(t) + B_i u_i(t) + G_i w_i(t - \tau_i) \tag{5}$$

$$y_i(t) = \left[x_i^T(t), w_i(t)\right]^T \tag{6}$$

where τ_i is the communication delay, $x_i(t) = [\delta_i \quad \Delta v_i \quad a_i]^T$ is the state of the system, $y_i(t) = [\delta_i \quad \Delta v_i \quad a_i \quad w_i(t)]^T$ is the output, and

$$A_i = \begin{bmatrix} 0 & 1 & -h \\ 0 & 0 & -1 \\ 0 & 0 & -1/\varsigma_i \end{bmatrix} \quad B_i = \begin{bmatrix} 0 \\ 0 \\ 1/\varsigma_i \end{bmatrix} \quad G_i = \begin{bmatrix} 0 \\ 1 \\ 0 \end{bmatrix}. \tag{7}$$

For each following vehicle, the kernel controller to be designed is in the form

$$u_i(t) \equiv u_i(t_k) = p_i y_i(t_k) \tag{8}$$

for $t \in (t_k, t_{k+1}]$, where $t_k = kT$, T is the sampling period, $k = 0, 1, 2, \ldots$, $p_i = [p_p \quad p_v \quad p_a \quad p_{ac}]$ is the controller gain vector to be determined.

Note that in the CACC setup, the control law is based on the spacing error (which can be calculated using the distance measurement) and the relative velocity between vehicle i and its preceding vehicle, the acceleration of vehicle i and vehicle $i-1$ (i.e., the proceeding vehicle). The first two quantities are measured by onboard sensors while the proceeding vehicle's acceleration is transmitted through a wireless communication channel.

B. Effect of Sensor Failures

As acceleration is measured by an accelerometer, which is insensitive to weather conditions, here, we consider the failure of the distance sensors and the relative velocity sensors. We adopt the general failure model in [27] to describe the failure in the distance and relative velocity sensors, i.e.,

$$\begin{aligned} \delta_i^f(t_k) &= \rho_{i\delta}\delta_i(t_k) \\ \Delta v_i^f(t_k) &= \rho_{iv}\Delta v_i(t_k) \end{aligned}$$

where $0 \leq \rho_{i\delta} \leq 1$ and $0 \leq \rho_{iv} \leq 1$ are the failure status.

Remark 1: Note that this sensor model can be divided into three cases: normal operation with $\rho_{i\delta}, \rho_{iv} = 1$, complete failure with $0 \leq \rho_{i\delta} < \underline{\rho}_{i\delta}$ and $0 \leq \rho_{iv} < \underline{\rho}_{iv}$, where $0 < \underline{\rho}_{i\delta} < 1$ and $0 < \underline{\rho}_{iv} < 1$ are the thresholds for complete failure, and partial failure with $\underline{\rho}_{i\delta} \leq \rho_{i\delta} < 1$ and $\underline{\rho}_{iv} \leq \rho_{iv} < 1$, which bridges over the former two cases.

Taking sensor failure effects into consideration, the controller input vector for vehicle i becomes

$$y_i^f(t_k) = \rho_i y_i(t_k) \tag{9}$$

where $y_i^f(t_k)$ is the output from the sensor that failed, and $\rho_i = \text{diag}\{\rho_{i\delta}, \rho_{iv}, 1, 1\}$ is the failure status matrix of the ith vehicle.

We now proceed to show how the sensor failures affect the CACC system. To this end, we first write the controller in (8) in the form of a digital controller, i.e.,

$$u_i(t_k) = p_{ix}x_i(t_k) + p_{iw}w_i(t_k - \tau_i) \tag{10}$$

where $p_{ix} = [p_p \quad p_v \quad p_a]$, $p_{iw} = p_{ac}$.

For simplicity, we introduce an indicator $\sigma(t) \in \{s, u\}$ to denote the sensor complete-failure states, namely, $\sigma(t) = u$ denotes complete sensor failure and $\sigma(t) = s$ otherwise. Then, the closed-loop CACC system in sampling interval $(t_k, t_{k+1}]$, $k = 0, 1, 2 \ldots$ can be written in the form

$$\begin{cases} S_{is} : \dot{x}_i(t) = A_i x_i(t) + B_i p_{ix}^s x_i(t_k) \\ \qquad\qquad + B_i p_{iw}^s w_i(t_k - \tau_i), & \sigma(t) = s \\ S_{iu} : \dot{x}_i(t) = A_i x_i(t) + B_i p_{ix}^u x_i(t_k) \\ \qquad\qquad + B_i p_{iw}^u w_i(t_k - \tau_i), & \sigma(t) = u \end{cases} \tag{11}$$

where $t \in (t_k, t_{k+1}]$.

Note that the control input is $u_i(t_k) = p_{ix}^u x_i(t_k) + p_{iw}^u w_i(t_k)$, where $p_{ix}^u = [0 \quad 0 \quad p_a \quad 0]$, $p_{iw}^u = [0 \quad 0 \quad 0 \quad p_{ac}]$, in the case where the onboard sensors completely fail (namely, $0 \le \rho_{i\delta} < \underline{\rho}_{i\delta}$ and $0 \le \rho_{iv} < \underline{\rho}_{iv}$); otherwise, for cases of normal operation and partial failure, i.e., $\underline{\rho}_{i\delta} \le \rho_{i\delta} \le 1$ and $\underline{\rho}_{iv} \le \rho_{iv} \le 1$, the control input is $u_i(t_k) = p_{ix}^s x_i(t_k) + p_{iw}^s w_i(t_k)$, where $p_{iw}^s = p_{iw}^u$, $p_{ix}^s = [p_p\rho_{i\delta} \quad p_v\rho_{iv} \quad p_a \quad 0]$. It is seen from (11) that the CACC system with sensor failures is essentially a switched system. In particular, in the complete-sensor-failure case, the system might become unstable due to inaccurate sensor output.

For the convenience of forthcoming discussion, here, we adopt the approach in [28] and [29] to transform the above hybrid system into a continuous one. Let us define $\tau(t_k) = t - t_k$ and suppose that the initial condition is $x(s) = \phi(s) = \phi(t_0)$ for $s \le t_0$. Then, system (11) can be rewritten as the following continuous-time switched delay system:

$$\dot{x}_i(t) = A_i x_i(t) + B_{ix}^{\sigma(t)} x_i(t - \tau(t_k)) + B_{iw}^{\sigma(t)} w_i(t - \tau(t_k) - \tau_i) \tag{12}$$

for $t \in (t_k, t_{k+1}]$, where $\sigma(t)$ serves as the switching signal, $B_{ix}^s = B_i p_{ix}^s$, $B_{iw}^s = B_i p_{iw}^s$, $B_{ix}^u = B_i p_{ix}^u$, and $B_{iw}^u = B_i p_{iw}^u$, $0 < \tau(t_k) \le T$.

Let t_s and t_u denote the total time during which the ith vehicle operates in modes s and u, respectively, over time interval $[t_0.t]$. Then, we have $t_s + t_u = t - t_0$. Define $\Delta_s = t_s/(t - t_0)$ and $\Delta_u = t_u/(t - t_0)$. Then, Δ_s and Δ_u are called the attention rate and the sensor complete-failure rate, respectively. It is clear that $\Delta_s + \Delta_u = 1$.

Remark 2: Note that when the onboard sensors work in a normal situation, the system in (12) is stable under the conditions given in [3]–[7]. Otherwise, if there are failures, system (12) is a continuous-time switched delay system with both stable and unstable subsystems S_s and S_u. This makes the problem rather challenging.

C. Objective

The objective of this research is to design a switched controller for the CACC system to maintain safe intervehicle spacing and to meet the following criteria.

(I) Individual vehicle stability: The entire closed-loop CACC system is exponentially stable.

(II) Steady-state performance: The relative velocity errors $\Delta v_i(t)$ approach zero for all vehicles.

(III) String stability [11]: The oscillations are not amplifying with the vehicle index due to any maneuver of the lead vehicle, namely, $\|G(jw)\| \le 1$ for any w, where $G(s) = a_i(s)/a_{i-1}(s)$ with $a_i(s)$ and $a_{i-1}(s)$ denotes the Laplace transforms of the acceleration $a_i(t)$ and $a_{i-1}(t)$, respectively.

Before giving the main results on controller design, we first give two definitions.

Definition 1: For any $\tau_2 > \tau_1 \ge 0$, let $N_{\sigma(\tau_1 \cdot \tau_2)}$ denote the number of switching of $\sigma(t)$ over $[\tau_1, \tau_2]$. If $N_{\sigma(\tau_1 \cdot \tau_2)} \le N_0 + (\tau_2 - \tau_1)/T_a$ holds for $T_a > 0$ and $N_0 \ge 0$, then T_a is called the average dwell time, and N_0 is the chatter bound. For simplicity, in this study, we choose $N_0 = 0$ [30].

Definition 2: CACC system (12) is said to be exponentially stable if there exists a constant $\lambda_i > 0 (i = 1, \ldots, n-1)$ for the ith vehicle, such that for any initial condition $\phi(t_0)$, the corresponding CACC system state satisfies $\|x_i(t)\| \le ce^{-\lambda_i(t - t_0)} \|\phi\|_m$, $\forall t \ge t_0$, where $\|\phi\|_m = \max\{\|\phi(t_0)\|, \|\dot{\phi}(t_0)\|\}$, and $c > 0$ is a constant, λ_i is called the decay rate.

III. Controller Design

Here, we give a set of sufficient conditions that can ensure that all the vehicles in the string are exponentially stable under the effect of sensor failures. By a closer inspection of these conditions, several interesting relations between the system decay rate, the sampling period, and the sensor complete-failure rate are obtained.

We first present the following proposition, which will play a key role in the main results.

Proposition 1: For given scalars $T > 0$, $\alpha_i^s > 0$ and $\alpha_i^u < 0$, if there exist matrices $P_i^j > 0$, $R_i^j > 0$, $Q_i^j > 0$, k_{ix}, k_{iw}, M_{i1}^j, M_{i2}^j, and M_{i3}^j, $j = s, u$, such that the matrix inequalities in (13), shown at the bottom of the next page, hold, where $C_{i1} = [0 \quad 0 \quad 0 \quad 1]^T$, $\varphi_i^s = 1$, and $\varphi_i^u = 0$, then

$$V_i^j(t) \le e^{-\alpha_i^j(t - t_0)} V_i^j(t_0). \tag{14}$$

Proof: See Appendix.

Remark 3: Note that if we define $c_i^j = \lambda_{\min}(P_i^j)$, $e_i^j = (T/\alpha_i^j - (1 - e^{-\alpha_i^j}/(\alpha_i^j)^2)$, $b_{pi}^j = \lambda_{\max}(P_i^j)$, $b_{qi}^j = \lambda_{\max}(Q_i^j)$, then $\|x_i(t)\| \le \sqrt{b_{pi}^j + e_i^j b_{qi}^j / c_i^j} e^{-0.5\alpha_i^j(t - t_0)} \|\phi\|_m$ follows from (14), where ϕ is the initial state defined before (12), which implies by Definition 1 that S_s is exponentially stable with decay rate $\lambda_i^s = 0.5\alpha_i^s$ and that the state increase rate of S_u is bounded by $\lambda_i^u = 0.5|\alpha_i^u|$.

Denote $T_1^+, \ldots, T_m^+$ as the switching instants of $\sigma(t)$ in the interval $[t_0, t)$, where $t_0 < T_1^+ < \cdots < T_m^+ < t$, $m \ge 1$. Here, T_n^+ is the time instant that is immediately after T_n, $n = 1, \ldots, m$, where T_n is the sampling instant and belongs to $\{t_1, t_2, \ldots\}$. Then, we give an exponential stability condition for the CACC system in the following theorem.

Theorem 1: For given scalars $T>0$, $\alpha_i^s>0$, $\alpha_i^u<0$, and $\mu_i>0$, the closed-loop CACC system in (12) is exponentially stable if there exist matrices $P_i^j>0, R_i^j>0, Q_i^j>0, p_{ix}, p_{iw}$, M_{i1}^j, M_{i2}^j, and M_{i3}^j, $j=s,u$, such that (13) and the following inequalities hold:

$$P_i^s-\mu_i P_i^u\le 0,\quad R_i^s-\mu_i R_i^u\le 0 \tag{15}$$
$$Q_i^s-\mu_i Q_i^u\le 0 \tag{16}$$
$$P_i^u-\mu_i e^{(\alpha_i^s-\alpha_i^u)T}P_i^s\le 0,\quad R_i^u-\mu_i R_i^s\le 0 \tag{17}$$
$$Q_i^u-\mu_i Q_i^s\le 0 \tag{18}$$
$$T_i^a>T_i^*=\ln\mu_i\varepsilon_i/\alpha_i^s. \tag{19}$$

Furthermore, the exponential decay rate is

$$\lambda_i=0.5\left(\eta_i-\ln\mu_i\varepsilon_i/T_i^a\right) \tag{20}$$

where $\varepsilon_i=e^{0.5T(\alpha_i^s-\alpha_i^u)}$, $\eta_i=\alpha_i^s-(\alpha_i^s-\alpha_i^u)\Delta_{ui}$, and T_i^a is the average dwell time of vehicle i, and the sensor complete-failure rate is upper bounded by

$$\Delta_{ui}<\Delta_{ui}^*=\left(\alpha_i^s-\left(\ln\mu_i\varepsilon_i/T_i^a\right)\right)/\left(\alpha_i^s-\alpha_i^u\right). \tag{21}$$

Proof: Define the following Lyapunov–Krasovskii functional for system (12):

$$\begin{aligned}V_i^{\sigma(t)}(t)=&\,x_i^T(t)P_i^{\sigma(t)}x_i(t)\\&+2\int_0^{t-\tau(t)-\tau_i}w_i^T(s)C_{i1}^TR_i^{\sigma(t)}C_{i1}w_i(s)\,ds\\&+\int_{-T}^{0}\int_{t+\theta}^{t}\dot{x}_i^T(s)e^{\alpha_i^{\sigma(t)}(s-t)}Q_i^{\sigma(t)}\dot{x}_i(s)\,ds\,d\theta.\end{aligned} \tag{22}$$

Bearing in mind that the states of system (12) do not jump at the switching instants and by applying (15) and (16), we get, when system (12) switches from S_u to S_s, that

$$\begin{aligned}V_i^s\left(T_n^+\right)=&\,x_i^T\left(T_n^+\right)P_i^sx_i\left(T_n^+\right)\\&+2\int_0^{T_n^+-\tau(t)-\tau_i}w_i^T(s)C_{i1}^TR_i^sC_{i1}w_i(s)\,ds\\&+\int_{-T}^{0}\int_{T_n^++\theta}^{T_n^+}\dot{x}_i^T(s)e^{\alpha_i^s(s-T_n^+)}Q_i^s\dot{x}_i(s)\,ds\,d\theta\\=&\,x_i^T(T_n)P_i^sx_i(T_n)\\&+2\int_0^{T_n-\tau(t)-\tau_i}w_i^T(s)C_{i1}^TR_i^sC_{i1}w_i(s)\,ds\\&+\int_{-T}^{0}\int_{T_n+\theta}^{T_n}\dot{x}_i^T(s)e^{\alpha_i^u(s-T_n)}e^{\left(\alpha_i^s-\alpha_i^u\right)(s-T_n)}\\&\times Q_i^s\dot{x}_i(s)\,ds\,d\theta\\\le&\,\mu_iV_i^u(T_n).\end{aligned} \tag{23}$$

When system (12) switches from S_s to S_u, we get, by applying (17) and (18), that

$$\begin{aligned}V_i^u\left(T_n^+\right)=&\,x_i^T\left(T_n^+\right)P_i^ux_i\left(T_n^+\right)\\&+2\int_0^{T_n^+-\tau(t)-\tau_i}w_i^T(s)C_{i1}^TR_i^uC_{i1}w_i(s)\,ds\\&+\int_{-T}^{0}\int_{T_n^++\theta}^{T_n^+}\dot{x}_i^T(s)e^{\alpha_i^u(s-T_n^+)}Q_i^u\dot{x}_i(s)\,ds\,d\theta\\=&\,x_i^T(T_n)P_i^ux_i(T_n)\\&+2\int_0^{T_n^+-\tau(t)-\tau_i}w_i^T(s)C_{i1}^TR_i^uC_{i1}w_i(s)ds\\&+\int_{-T}^{0}\int_{T_n+\theta}^{T_n}\dot{x}_i^T(s)e^{\alpha_i^s(s-T_n)}e^{\left(\alpha_i^u-\alpha_i^s\right)(s-T_n)}\\&\times Q_i^u\dot{x}_i(s)\,ds\,d\theta\\\le&\,\mu_ie^{(\alpha_i^s-\alpha_i^u)T}V_i^s(T_n).\end{aligned} \tag{24}$$

Let

$$\chi=\begin{cases}\mu_i & S_u\to S_s\\ \mu_ie^{(\alpha_i^s-\alpha_i^u)T} & S_s\to S_u.\end{cases}$$

Then, (23) and (24) are rewritten as

$$V_i^{\sigma\left(T_n^+\right)}\left(T_n^+\right)\le\chi V_i^{\sigma(T_n)}(T_n). \tag{25}$$

Denote the number of $S_u\to S_s$ and that of $S_s\to S_u$ over the interval $[t_0,t]$ as π_{us} and π_{su}, respectively. Then, by following the timing analysis of the switching signal, we have

$$\begin{aligned}\Omega_i^j\triangleq&\begin{bmatrix}A_i^TP_i^j+P_i^jA_i+\alpha_i^jP_i^j+(M_{i1}^j)^T+M_{i1}^j & \left(B_{ix}^j\right)^TP_i^j-\left(M_{i1}^j\right)^T+M_{i2}^j & \left(B_{iw}^j\right)^T+M_{i3}^j\\ * & -\left(M_{i2}^j\right)^T-M_{i2}^j & -M_{i3}^j\\ * & * & C_{i1}^TR_i^j\end{bmatrix}\\&+\begin{bmatrix}A_i^T\\ \left(B_{ix}^j\right)^T\\ \left(B_{iw}^j\right)^T\end{bmatrix}TQ_i^j\begin{bmatrix}A_i & B_{ix}^j & B_{iw}^j\end{bmatrix}+T\begin{bmatrix}\left(M_{i1}^j\right)^T\\ \left(M_{i2}^j\right)^T\\ \left(M_{i3}^j\right)^T\end{bmatrix}\left(e^{-\alpha_i^j\varphi_i^j}Q_i^j\right)^{-1}\begin{bmatrix}M_{i1}^j & M_{i2}^j & M_{i3}^j\end{bmatrix}<0\end{aligned} \tag{13}$$

$\pi_{us} \le \pi_{su} + 1$ and $\pi_{us} + \pi_{su} = N_\sigma(t, t_0)$, which yields $\pi_{su} \le (N_\sigma(t, t_0) + 1)/2$. It follows from the given inequality that

$$e^{\left(\alpha_i^s - \alpha_i^u\right) T \pi_{su}} \le \varepsilon_i \times \varepsilon_i^{N_\sigma(t,t_0)}. \tag{26}$$

According to Lyapunov–Krasovskii functional (22), we get, by applying (14), (25), (26), and Definition 1, that

$$\begin{aligned}
V_i^{\sigma(t)}(t) &\le e^{-\alpha_i^{\sigma\left(T_m^+\right)}\left(t - T_m^+\right)} V_i^{\sigma\left(T_m^+\right)}\left(T_m^+\right) \\
&\le e^{-\alpha_i^{\sigma\left(T_m^+\right)}\left(t - T_m^+\right)} \chi V_i^{\sigma(T_m)}(T_m) \le \cdots \\
&\le \mu_i^{N_\sigma(t,t_0)} e^{\left(\alpha_i^s - \alpha_i^u\right) T \pi_{us}} e^{-\alpha_i^{\sigma\left(T_m^+\right)}\left(t - T_m^+\right)} \\
&\quad \times e^{-\alpha_i^{\sigma\left(T_{m-1}^+\right)}\left(T_m - T_{m-1}^+\right)} \\
&\quad \cdots e^{-\alpha_i^{\sigma\left(T_1^+\right)}\left(T_2 - T_1^+\right)} e^{-\alpha_i^{\sigma\left(T_0^+\right)}\left(T_1 - T_0^+\right)} \\
&\quad \times V_i^{\sigma\left(T_0^+\right)}\left(t_0^+\right) \\
&\le \varepsilon_i (\mu_i \varepsilon_i)^{N_\sigma(t,t_0)} e^{-\alpha_i^s t_s} e^{-\alpha_i^u t_u} V_i^{\sigma\left(t_0^+\right)}\left(t_0^+\right) \\
&\le \varepsilon_i (e^{\ln \mu_i \varepsilon_i / T_i^a})^{(t-t_0)} \left(e^{-\alpha_i^s t_s/(t-t_0)}\right)^{(t-t_0)} \\
&\quad \times \left(e^{-\alpha_i^u t_u/(t-t_0)}\right)^{(t-t_0)} V_i^{\sigma\left(t_0^+\right)}\left(t_0^+\right) \\
&= \varepsilon_i \left(e^{\ln \mu_i \varepsilon_i / T_i^a}\right)^{(t-t_0)} \left(e^{-\alpha_i^s \Delta_s}\right)^{(t-t_0)} \\
&\quad \times \left(e^{-\alpha_i^s \Delta_u}\right)^{(t-t_0)} V_i^{\sigma\left(t_0^+\right)}\left(t_0^+\right) \\
&= \varepsilon_i e^{-2\lambda_i (t-t_0)} V_i^{\sigma(t_0)}(t_0).
\end{aligned} \tag{27}$$

Let $c_i = \min\{c_i^s, c_i^u\}$, $b_{pi} = \max\{b_{pi}^s, b_{pi}^u\}$, $b_{qi} = \max\{b_{qi}^s, b_{qi}^u\}$, and $e_i = \max\{e_i^s, e_i^u\}$. Then, we get from (27) that

$$\begin{aligned}
c_i \left\|x_i(t)\right\|^2 &\le V_i^{\sigma(t)}(t) \le \varepsilon_i e^{-2\lambda_i (t-t_0)} V_i^{\sigma(t_0)}(t_0) \\
&\le \varepsilon_i (b_{pi} + b_{qi} e_i) e^{-2\lambda_i (t-t_0)} \|\phi\|_m^2
\end{aligned} \tag{28}$$

which yields

$$\|x_i(t)\| \le \sqrt{\varepsilon_i (b_{pi} + b_{qi} e_i)/c_i}\, e^{-2\lambda_i (t-t_0)} \|\phi\|_m. \tag{29}$$

Equation (19) implies that $\lambda_i > 0$. Hence, it follows from (29) and Definition 2 that CACC system (12) with sensor failures is exponentially stable with decay rate λ_i. The proof is completed.

From Theorem 1, we can derive the quantitative relations among the exponential decay rate, the sensor complete-failure rate, the sampling period, and the admissible sensor complete-failure rate bound, which can be given in the following corollary without proof.

Corollary 1: If parameters α_i^s, α_i^u, μ_i, and T_i^a in (20) are given, then the admissible sensor complete-failure rate bound Δ_{ui}^* and the sampling period T satisfy

$$\Delta_{ui}^*(T) = -0.5T/T_i^a + \left(\alpha_i^s - \ln \mu_i / T_i^a\right) / \left(\alpha_i^s - \alpha_i^u\right). \tag{30}$$

If sampling period T is also given, the exponential decay rate λ_i and the sensor complete-failure rate Δ_{ui} have the relationship

$$\begin{aligned}
\lambda_i(\Delta_{ui}) = 0.5\alpha_i^s - 0.5\left(\alpha_i^s - \alpha_i^u\right)\Delta_{ui} \\
- \left[0.25T\left(\alpha_i^s - \alpha_i^u\right) + 0.5 \ln \mu_i\right] / T_i^a.
\end{aligned} \tag{31}$$

If the sensor complete-failure rate Δ_{ui} is known, the exponential decay rate λ_i is determined by sampling period T as

$$\begin{aligned}
\lambda_i(T) = -0.25\left(\alpha_i^s - \alpha_i^u\right) T/T_i^a \\
+ 0.5\left[\alpha_i^s - \left(\alpha_i^s - \alpha_i^u\right)\Delta_{ui} - \ln \mu_i / T_i^a\right].
\end{aligned} \tag{32}$$

Remark 4: It can be seen from (32) and (30) that a larger sampling period of the vehicle can yield a smaller admissible sensor complete-failure rate bound and exponential decay rate for the CACC system. Hence, we can improve the robustness of the system by reducing the sampling period. It follows from (31) that the larger the sensor complete-failure rate, the worse the stability performance. That is to say, we may judge the stability of the CACC system in advance when the sensor complete-failure rate is known.

Theorem 1 supplies a sufficient condition for the CACC system to be exponentially stable. We now proceed to discussing a stabilizing controller design method in the following theorem.

Theorem 2: For given scalars $T > 0$, $\alpha_i^s > 0$, $\alpha_i^u < 0$, and $\mu_i > 0$, the closed-loop CACC system in (12) is exponentially stable if there exist matrices $R_i^j > 0$, $Z_i^j > 0$, V_i^j, N_{i1}^j, N_{i2}^j, and N_{i3}^j, $j = s, u$, such that (21) and the linear matrix inequalities in (33)–(36), shown at the bottom of the page, hold, where

$$\begin{bmatrix}
\Phi_{i1} & B_i^j V_i^j - \left(N_{i1}^j\right)^T + N_{i2}^j & B_i^j W_i^j + N_{i3}^j & Y_i^j A_i^T & (N_{i1}^j)^T \\
* & -\left(N_{i2}^j\right)^T - N_{i2}^j & -N_{i3}^j & \left(V_i^j\right)^T \left(B_i^j\right)^T & \left(N_{i2}^j\right)^T \\
* & * & Y_i^j C_{i1}^T & \left(W_i^j\right)^T \left(B_i^j\right)^T & \left(N_{i3}^j\right)^T \\
* & * & * & -T^{-1} Z_i^j & 0 \\
* & * & * & * & -T^{-1} e^{-\alpha_i^j \varphi_i^j}\left(2Y_i^j - Z_i^j\right)
\end{bmatrix} > 0 \tag{33}$$

$$\begin{bmatrix} -\mu_i Y_i^u & Y_i^u \\ * & -Y_i^s \end{bmatrix} \le 0, \quad \begin{bmatrix} -\mu_i e^{\left(\alpha_i^s - \alpha_i^u\right) T} Y_i^s & Y_i^s \\ * & -Y_i^u \end{bmatrix} \le 0 \tag{34}$$

$$\begin{bmatrix} -\mu_i U_i^u & U_i^u \\ * & -U_i^s \end{bmatrix} \le 0, \quad \begin{bmatrix} -\mu_i U_i^s & U_i^s \\ * & -U_i^u \end{bmatrix} \le 0 \tag{35}$$

$$\begin{bmatrix} -\mu_i Z_i^u & Z_i^u \\ * & -Z_i^s \end{bmatrix} \le 0, \quad \begin{bmatrix} -\mu_i Z_i^s & Z_i^s \\ * & -Z_i^u \end{bmatrix} \le 0 \tag{36}$$

$\Phi_{i1} = A_i^T Y_i^j + Y_i^j A_i + \alpha_i^j Y_i^j + (N_{i1}^j)^T + N_{i1}^j$, the sensor complete-failure rate upper bound Δ_{ui}^*, the decay rate λ_i, and the average dwell time T_i^a are given in Theorem 1. Furthermore, the controller gains can be given by

$$p_{ix}^s = V_i^j \left(Y_i^j\right)^{-1} \qquad p_{iw}^s = W_i^j \left(U_i^j\right)^{-1}. \tag{37}$$

Proof: By Schur complement, $\Omega_i^j < 0$ is equivalent to inequality

$$\begin{bmatrix} \Phi_{i2} & \Phi_{i3} & \Phi_{i4} & A_i^T & \left(M_{i1}^j\right)^T \\ * & -\left(M_{i2}^j\right)^T & -M_{i2}^j & \left(B_{ix}^j\right)^T & \left(M_{i2}^j\right)^T \\ * & * & C_{i1}^T R_i^j & \left(B_{iw}^j\right)^T & \left(M_{i3}^j\right)^T \\ * & * & * & -T^{-1}\left(Q_i^j\right)^{-1} & 0 \\ * & * & * & * & -T^{-1} e^{-\alpha_i^j \varphi_i^j} Q_i^j \end{bmatrix} < 0 \tag{38}$$

where

$$\begin{aligned} \Phi_{i2} &= A_i^T P_i^j + P_i^j A_i + \alpha_i^j P_i^j + \left(M_{i1}^j\right)^T + M_{i1}^j \\ \Phi_{i3} &= \left(B_{ix}^j\right)^T P_i^j - \left(M_{i1}^j\right)^T + M_{i2}^j \\ \Phi_{i4} &= \left(B_{iw}^j\right)^T P_i^j + M_{i3}^j. \end{aligned}$$

Denote $Y_i^j = (P_i^j)^{-1}$, $Z_i^j = (Q_i^j)^{-1}$, $U_i^j = (R_i^j)^{-1}$, $V_i^j = p_{ix}^s Y_i^j$, $W_i^j = p_{iw}^s U_i^j$, $N_{i1}^j = Y_i^j M_{i1}^j Y_i^j$, $N_{i2}^j = Y_i^j M_{i2}^j Y_i^j$, and $N_{i3}^j = Y_i^j M_{i3}^j U_i^j$. Multiplying both sides of (38) by $\mathrm{diag}\{Y_i^j, Y_i^j, U_i^j, Y_i^j, Y_i^j\}$ and applying the inequality $Y_i^j Q_i^j Y_i^j \geq 2Y_i^j - (Q_i^j)^{-1}$ yield (33). Multiplying both sides of (15) and (18) by Y_i^u and Y_i^s, respectively, and applying Schur complement yield (34). Similarly, multiplying both sides of (16) and (19) by $(Z_i)_u$ and Z_i^s and (17) and (20) by U_i^u and U_i^s, respectively, leads to inequalities (35) and (36). Using (12), we obtain the controller gains $p_{ix} = V_i^j (Y_i^j)^{-1}$ and $p_{iw} = W_i^j (U_i^j)^{-1}$. Then, from Theorem 1, we can easily prove Theorem 2.

Remark 5: One may question: Why not use the Routh–Hurwitz test for stability analysis and controller design here? Sure, we can realize this [using the Routh–Hurwitz test and the transfer function in (44)], and the controllers resulted can stabilize the single vehicles in either case of sensor failure and normal operation. However, when frequent sensor failure-normal switching happens, such controllers cannot guarantee single vehicle stability. The reason lies in the fact that involving the switching dynamics into the Routh–Hurwitz stability test to yield a feasible solution is not easy, if not infeasible. For this reason, here, we choose to address this problem using switching systems theory. The presented method is also preferable because we can easily uncover the connections between the system decay rate, the sensor complete-failure rate, and the sampling period (see Corollary 1).

IV. String Stability and Control Algorithm

In the previous section, considerations have been primarily focused on exponential stability of all the individual vehicles in the CACC system. This section is concerned with the issue of string stability, which is associated with objectives 1) and 3) given in Section II-C. Here, we first give a result on string stability and then derive an additional set of constraints to guarantee a zero steady-state velocity error. The analysis and results are based on the sampled-data controller (37) previously obtained.

Theorem 3: The closed-loop CACC system (12) is string stable if the following conditions are satisfied:

$$\begin{cases} K_{px} \geq 0 \\ \varsigma^2 + (p_a + \varsigma h K_{px} + K_{vx})\tau_i^2 + p_a K_{vx} \tau_i^3/3 \geq 0 \\ (p_a - 1)^2 - 2\varsigma h K_{px} - 2\varsigma K_{vx} - p_{ac}^2 - 2p_{ac} K_{vx} \tau_i \\ \quad + p_{ac} K_{px} \tau_i^2 \geq 0 \\ 2(p_a - 1) + h^2 K_{px} + 2K_{vx} + p_{ac} = 0. \end{cases} \tag{39}$$

Proof: Suppose each following vehicles in the CACC system is under control of the switched controller (10). Substituting (8) and (10) into (4), we obtain

$$\begin{aligned} \dot{a}_i(t) = -a_i(t)/\varsigma_i + [K_{px}\delta_i(t) + K_{vx}(\Delta v_i(t)) \\ + p_a a_i(t) + p_{ac} a_{i-1}(t - \tau_i)]/\varsigma_i \end{aligned} \tag{40}$$

where $K_{px} = K_{vx} = 0$ when the sensor completely fails and $K_{px} = \rho_{i\delta} p_p$, $K_{vx} = \rho_{iv} p_v$ otherwise. Taking Laplace transformation to the equation in (40) and assuming that $a_i(0) = 0$, we can get

$$\begin{aligned} &\left[s - \left(\frac{p_a - 1}{\varsigma_i}\right)\right] a_i(s) \\ &\quad = \frac{1}{\varsigma_i}\left(K_{px}\delta_i(s) + K_{vx}\Delta v_i(s) + p_{ac} a_{i-1}(s) e^{-\tau_i s}\right). \end{aligned} \tag{41}$$

By using (1), we can have

$$\delta_i(s) = \frac{a_{i-1}(s) - a_i(s)}{s^2} - \frac{h a_i(s)}{s} \tag{42}$$

$$\Delta v_i(s) = \frac{a_{i-1}(s) - a_i(s)}{s}. \tag{43}$$

Substituting (42) and (43) into (41) and collecting similar terms together, we have

$$\begin{aligned} G(s) &= \frac{a_i(s)}{a_{i-1}(s)} \\ &= \frac{p_{ac} s^2 e^{-\tau_i s} + s K_{vx} + K_{px}}{s^3 \varsigma_i - s^2(p_a - 1) + s(h K_{px} + K_{vx}) + K_{px}}. \end{aligned} \tag{44}$$

If we impose the condition $|a_i(jw)/a_{i-1}(jw)| \leq 1$ for any w, then we can obtain the following inequality of w:

$$\begin{aligned} &w^4 \varsigma^2 + \left[1 + p_a^2 - p_{ac}^2 - 2p_a - \varsigma h K_{px} - 2K_{vx}\right] w^2 \\ &\quad - 2K_{vx} p_{ac} \sin(\tau_i w) w - K_{vx}^2 + 2p_{ac} K_{px} \cos(\tau_i w) \\ &\quad + 2K_{px} p_a + (h K_{px} + K_{vx})^2 - 2K_{px} \geq 0. \end{aligned} \tag{45}$$

By using second-order Taylor approximations, we have $\sin(\tau_i w)\approx\tau_i w-(\tau_i w)^3/3!$, $\cos(\tau_i w)\approx 1-(\tau_i w)^2/2!$. Then, (45) can be rewritten as

$$\begin{aligned}&\left[\varsigma^2+(p_a+\varsigma hK_{px}+K_{vx})\tau_i^2+p_aK_{vx}\tau_i^3/3\right]w^4\\&+\left[(p_a-1)^2-2\varsigma hK_{px}-2\varsigma K_{vx}-p_{ac}^2\right.\\&\quad\left.-2p_{ac}K_{vx}\tau_i+p_{ac}K_{px}\tau_i^2\right]w^2\\&+2K_{px}(p_a-1)+h^2K_{px}^2+2(K_{px}K_{vx}+K_{px}p_{ac})\geq 0.\end{aligned}$$

Therefore, if $K_{px}\geq 0$, then a sufficient condition for the nonnegativity of the fourth-order polynomial on the left-hand side of (45) is that

$$\begin{aligned}&\varsigma^2+(p_a+\varsigma hK_{px}+K_{vx})\tau_i^2+p_aK_{vx}\tau_i^3/3\geq 0,\\&(p_a-1)^2-2\varsigma hK_{px}-2\varsigma K_{vx}-p_{ac}^2\\&\quad-2p_{ac}K_{vx}\tau_i+p_{ac}K_{px}\tau_i^2\geq 0\\&2(p_a-1)+h^2K_{px}+2K_{vx}+p_{ac}=0.\end{aligned}$$

This completes the proof.

In what follows, we will show that a zero steady-state velocity error can be guaranteed by the presented controller. Let υ_0 denote the deviation of the first vehicle's acceleration from its steady-state value a_0 at time t, i.e., $\upsilon_0(t)=a_0(t)-a_0$. From (1), we have

$$\ddot{\delta}_1=\dot{\upsilon}_0-\dot{a}_1-h\ddot{a}_1. \tag{46}$$

Substituting (40) into (46) with $i=1$, we have

$$\begin{aligned}\dddot{\delta}_1(t)&=\dot{\upsilon}_0+(1+h\vartheta)\upsilon_0(t)-(\vartheta+h\vartheta^2-h\vartheta)\\&\times\left(K_{px}\delta_1(t)+K_{vx}\left(\Delta v_1(t)\right)+p_a\upsilon_0(t)+p_{ac}\upsilon_0(t)\right)\end{aligned} \tag{47}$$

which is the relative velocity error equation of the first following vehicle. Taking Laplace transformation of both sides of (47), we can describe the relative velocity error of the first follower with respect to the lead vehicle's speed change as in (48), shown at the bottom of the page. Suppose the lead vehicle can reach its final steady-state value within a finite time t_f. We have $\upsilon_0(t)-\upsilon_0(t_f)=0$ for all $t\geq t_f$. Thus, we can get

$$\upsilon_0(s)=\frac{\upsilon_0(t_f)}{s}. \tag{49}$$

By using the final value theorem and (47)–(49), we obtain that $\lim_{t\to\infty}\Delta v_i(t)=\lim_{s\to 0}sF^{i-1}(s)\Delta v_1(s)=0$, namely, a zero steady-state velocity error is achieved for vehicle i, $i=1,2,\ldots,n-1$.

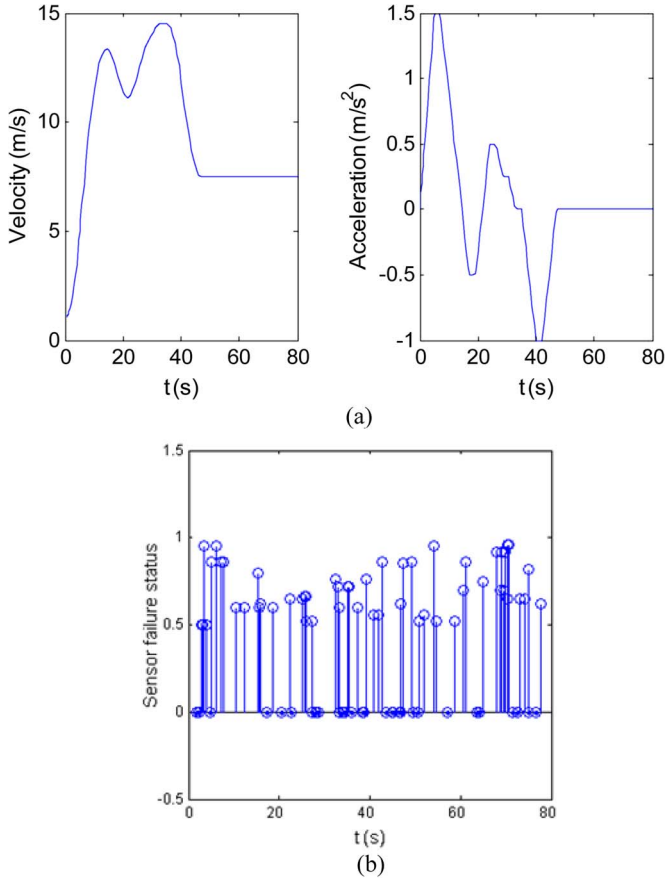

Fig. 3. (a) Profile of the lead vehicle. (b) Sensor failure status.

Finally, based on the given discussions and all the results established heretofore, we are in a position to give the following CACC algorithm.

Algorithm 1. The switched CACC control algorithm:

1) Design the feedback-linearization controller in (3), which is a routine procedure.

2) According to Theorem 3, we can derive $K_{px}\geq 0$, $K_{vx}\geq 0$, and $p_{ac}\geq 0$ and then choose a small initial value of α_i^s such that (21) is feasible.

3) Increase α_i^s by a certain step length $\Delta\alpha_i^s$ and test the feasibility of (21). If (21) is feasible, continue to increase α_i^s. Otherwise, exit and set $\alpha_i^s=\alpha_i^s-\Delta\alpha_i^s$.

4) Applying similar procedures as in steps 2) and 3) to derive the maximal α_i^u.

5) Choose a large μ_i such that Theorem 2 holds. Decrease μ_i by a certain step length $\Delta\mu_i$, if the conditions in Theorem 2 hold and then continue to decrease μ_i; otherwise, exit and set $\mu_i=\mu_i+\Delta\mu_i$.

$$F(s)=\frac{\Delta v_1(s)}{v_0(s)}=\frac{s^3+s^2+\left((1+h\vartheta)-(\vartheta+h\vartheta^2-h\vartheta)(p_a+p_{ac}e^{-\tau_i s})s+(\vartheta+h\vartheta^2-h\vartheta)K_{px}h\right)}{s^3+K_{px}s+(\vartheta+h\vartheta^2-h\vartheta)K_{px}} \tag{48}$$

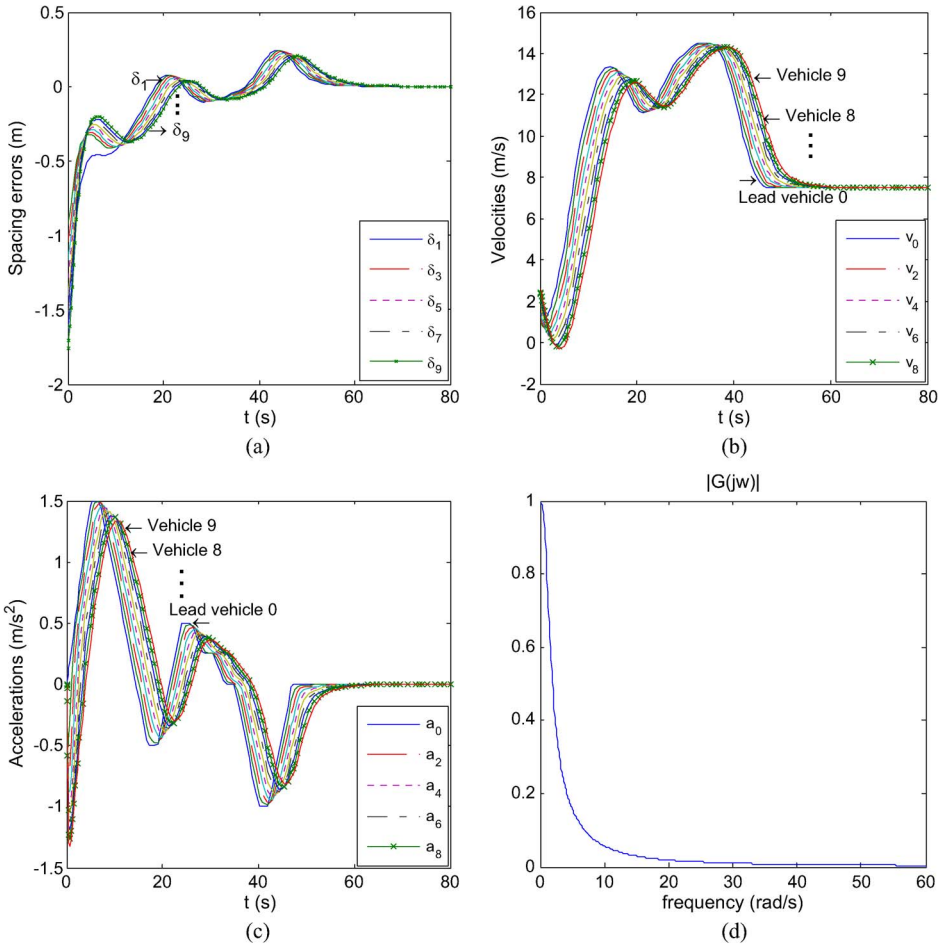

Fig. 4. Ten-vehicle CACC system under the presented switched controller: responses and spacing propagation characteristics. (a) Spacing errors. (b) Velocities. (c) Accelerations. (d) Frequency response $\exists w : |\mathrm{G(jw)}| \leq 1$.

V. Simulations and Experiments

A. Numerical Simulations

Here, we show via a numerical example how to apply the proposed control method to a ten-vehicle CACC system, which runs in a virtual environment established using System Build software package in MATLAB. Comparisons are made between the new method and the method in [32]. The profile of the lead vehicle's velocity and acceleration used in the simulations are shown in Fig. 3(a). The following parameters are used in the simulations: minimum vehicle distance $d_0 = 3$ m, length of vehicle $L_i = 4$ m, engineer time constant $\varsigma_i = 0.25$, and time gap $h = 0.7$. The other parameters used in the simulations are the same as those in [26], namely, specific mass of the air $\sigma = 1.2\,\mathrm{kg/m^3}$, cross-sectional area of the vehicle $A_i = 2.2\,\mathrm{m^2}$, drag coefficient $c_{di} = 0.35$, vehicle mass $m_i = 1464$ kg, and mechanical drag $d_{mi} = 5$ N. Substituting these parameters into (2) yields

$$\dot{a}_i = -4\left(a_i + 0.588v_i^2/1464 + 5/1464\right) - 1.104a_iv_i/1464 + c_i/366 \quad (50)$$

for which the feedback linearization controller in (3) is

$$c_i = 1464u_i + 0.588v_i^2 + 5 + 0.276\dot{v}_iv_i. \quad (51)$$

The trajectories of the ten vehicles and the spacing propagation characteristics denoted by $|G(jw)|$ are shown in Fig. 4, which are obviously superior to those in [32] (shown in Fig. 5). The sampling period is $T = 0.1$ s. In the simulation, we suppose that all the following vehicles have the same sensor failure status, namely, $\rho_{i\delta} = \rho_{iv} = \rho$. We use a random sequence $\sigma \in \{0 < \rho < 0.5, 0.5 \leq \rho < 1, \rho = 1\}$ to describe the sensor operating mode over time interval [0, 80 s], as shown in Fig. 3(b), which only plots the partial-failure status ($0.5 \leq \rho < 1$ with probability 0.07) and the complete-failure status ($0 \leq \rho < 0.5$ with probability 0.03). The average dwell time of each vehicle is $T_i^a = 1.6666$ s. According to Algorithm 1, when $\alpha_i^s = 0.41$, $\alpha_i^u = -0.39$, and $\mu_i = 2.11$, we have $T_i^* = 1.2222 < T_i^a$ and $\Delta_{ui}^* = 10.16\% > \Delta_{ui}$. Assume that the initial condition is $\delta_i = 0.2$ m, $\Delta v_i = 0.2$ m/s, and $a_i = 0$. Then, from Theorem 3 and Theorem 2, the controller gains are obtained as

$$p_{ix}^s = [0.540 \quad 1.531 \quad -0.218 \quad 0] \quad p_{iw}^s = [0 \quad 0 \quad 0 \quad 1.218].$$

In facing of an onboard sensor failure, the CACC system achieves tracking control accurately, with the maximum spacing error and acceleration being 0.23 m and 1.5 m/s^2, respectively. In this same case, when the method suggested in [32] is

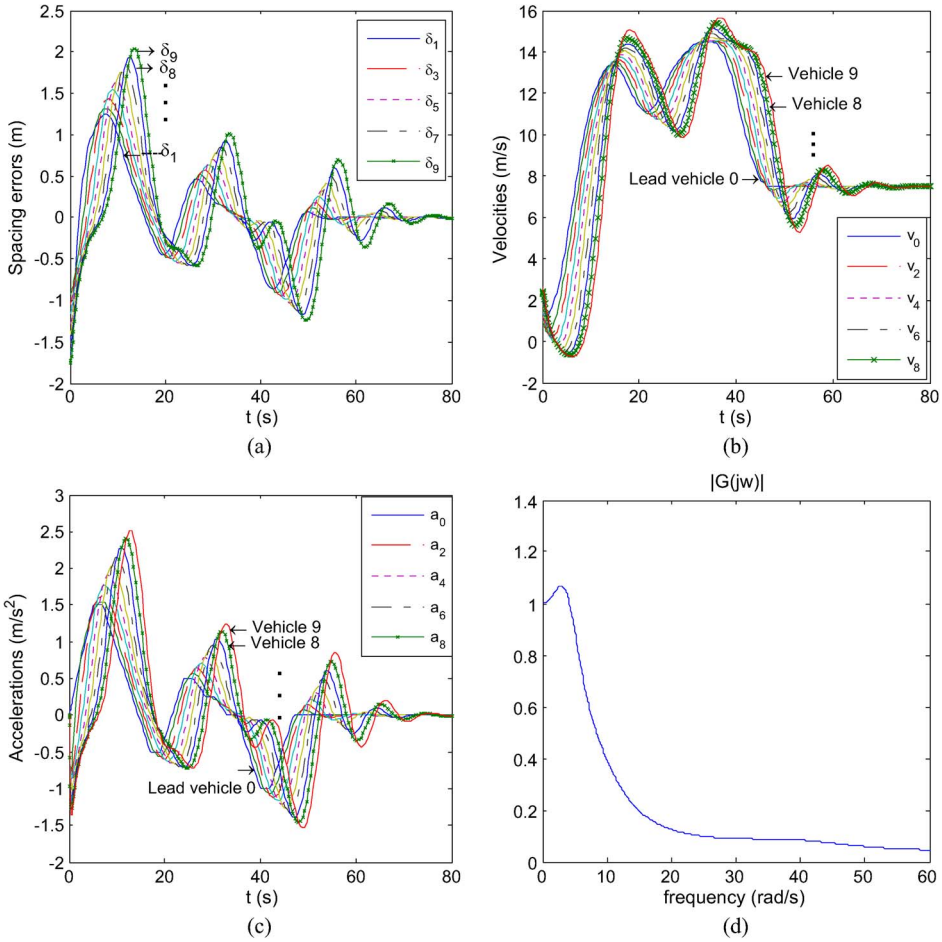

Fig. 5. Ten-vehicle CACC: system under controller [32]: responses and spacing propagation characteristics. (a) Spacing errors. (b) Velocities. (c) Accelerations. (d) Frequency response $\exists w|\mathrm{G(jw)}| > 1$.

used, the feedback/forward controller gains are obtained as

$$K_{i,i-1} = [0 \quad 0 \quad 0 \quad 0],\ K_{i,i} = [0 \quad 0 \quad 0 \quad -1] \text{ for } \rho = 0;$$

$$K_{i,i-1} = [0.0625 \quad 0.25 \quad 0 \quad 0]$$

$$K_{i,i} = [0.0625 \quad 0.2937 \quad 0.175 \quad -1] \text{ for } \rho = 1;$$

$$K_{i,i-1} = [0.0625\rho \quad 0.25\rho \quad 0 \quad 0]$$

$$K_{i,i} = [0.0625\rho \quad 0.2937\rho \quad 0.175\rho \quad -1] \text{ for } \rho = 0.9.$$

The system under these controllers is string unstable (see Fig. 5; particularly when complete failure of the onboard sensors happens). The maximum spacing and acceleration are 2.21 m and 2.52 m/s^2, respectively, which are much higher than in our case in Fig. 4(a) and (b). Moreover, note that $|G(jw)|$ in Fig. 4(d) satisfies the CACC objective 3) given in Section II.

In the same situation, the relations between decay rate λ_i, sensor complete-failure rate Δ_{ui}, admissible bound of sensor complete-failure rate Δ_{ui}^*, and sampling period T are investigated.

For $\alpha_i^s = 0.41$, $\alpha_i^u = -0.39$, $\mu_i = 2.11$, and $T_i^a = 1.6666$ s, the relation between T and Δ_{ui}^* is shown in Fig. 6(a). Furthermore, given $\Delta_{ui} = 3\%$, the relation between the sampling period and exponential decay λ_i is given in Fig. 6(b). The simulations show that λ_i decreases when T increases. Specially, λ_i decreases from 0.1005 to 0.0098 when T increases from 0.05 to 0.8055. If T increases to 0.9, λ_i decreases to -0.0015, which violates the basic fact of $\lambda_i > 0$. Thus, we know that, to guarantee the stability of the CACC system, the maximal sampling period is around 0.6 s. For $\alpha_i^s = 0.41$, $\alpha_i^u = -0.39$, $\mu_i = 2.11$, and $T_i^a = 1.6666$ s and $T = 0.1$ s, the relation between λ_i and sensor complete-failure rate Δ_{ui} is shown in Fig. 6(b). The results show that λ_i decreases when the sensor complete-failure rate increases. Specially, λ_i decreases from 0.0477 to 0.0199 when Δ_{ui} increases from 0.56% to 4.4%. If Δ_{ui} increases to 5%, λ_i decreases to -0.0021, and $\lambda_i > 0$ is not satisfied. Thus, we know that the maximal sensor complete-failure rate appears between 4.4% and 5%.

It is worth mentioning that in the given simulations, almost no fluctuation is visible in figures showing the spacing error, the velocity, and the acceleration of vehicles under the sensor failure profile in Fig. 3(b). This is desirable for a safe and comfortable driving experience. On the other hand, we must admit that the "smooth" vehicle performance is not achieved without cost. In fact, frequent fluctuations in response to sensor status switching do exist in the control signals (which are not plotted due to space limitations).

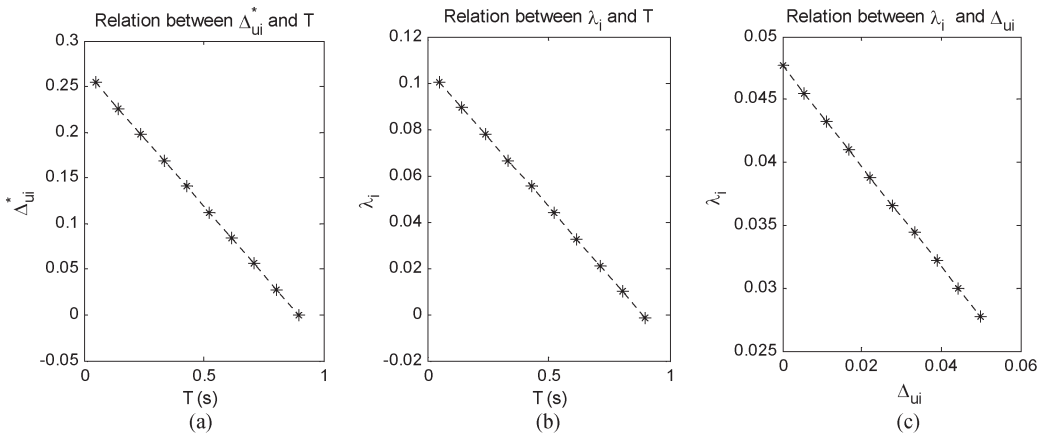

Fig. 6. Trajectories of functions. (a) λ_i and Δ_{ui}. (b) λ_i and T. (c) Δ_{ui}^* and T.

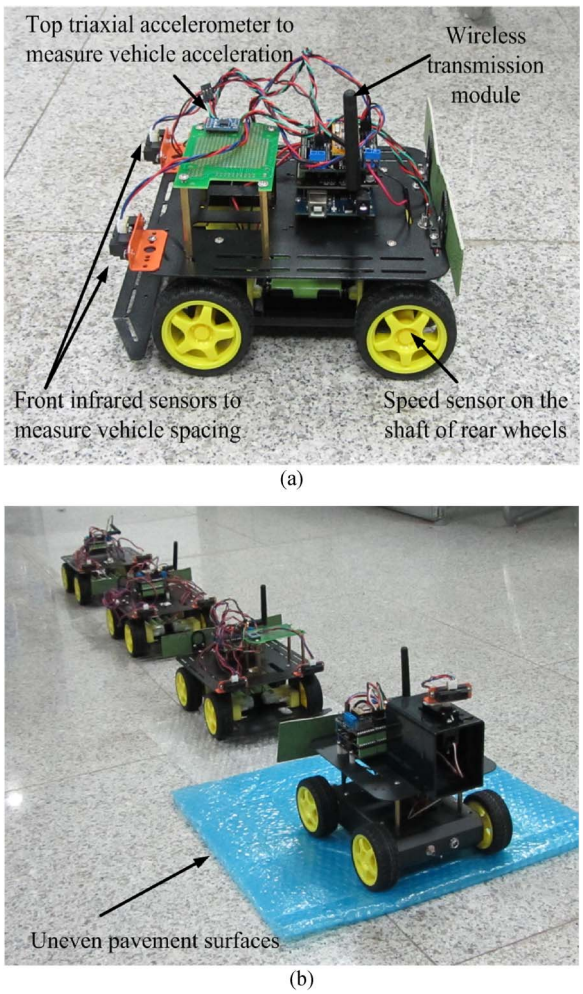

Fig. 7. (a) Arduino car. (b) Arduino CACC in experiment.

TABLE I
PARAMETERS OF THE FOUR ARDUINO CARS

$A_1/A_2/A_3/A_4$	15/12/12/12	cm^2
$d_{mi}/d_{mi}/d_{mi}/d_{mi}$	0.5/0.4/0.4/0.4	N
σ	0.98	m/s^3
c_{di}	0.15	----

B. Experiments

The simulations in the previous sections indicate that the proposed controller is simple in structure and that the parameters are easy to tune so that it can be quickly calibrated for a specific vehicle and can meet real-time requirements. Here, experimental studies are carried out to demonstrate some properties of the proposed controller. The experiments are based on four RF-controlled Arduino cars, shown in Fig. 7(a) and (b), which are driven and steered by two front wheels. Two infrared sensors are used to measure the distance between the following vehicle and the preceding vehicle. In the experiment, the relative velocity is estimated by distance error; hence, they have the same failure status. The complete-failure rates of the distance sensors for the three following Arduino cars are 3.5%, 3.9%, and 4.1%, respectively, and the partial-failure status is 0.96, which are identified using operational data. The sampling period is 0.2 s. Longitudinal speed and acceleration are detected by an incremental encoder sensor installed on the shaft of the rear wheels and an acceleration sensor installed on top of the vehicle, respectively. The relevant parameters of the Arduino cars are shown in Table I. An Arduino processor acts as the real-time computing and control unit. Fig. 8 shows the spacing and the velocity of the vehicles under control of the switched controller, wherein the desired spacing is 15 cm.

The first and most important objective of the experiment is to show the effectiveness of the presented method in dealing with sensor failures. The experiment results are depicted in Figs. 8 and 9. We can see in Fig. 8(a) that the presented controller performs well, and the maximum spacing error is 5.2 cm (caused by the acceleration of the lead vehicle). All the following vehicles accurately track the trajectory of their preceding vehicles [shown in Fig. 8(b)], and the objectives in Section II-C are achieved. However, the strategy in [32] renders the spacing to amplify downstream along the CACC system when complete failure happens, i.e., string instability appears, and the maximum spacing error is 7.4 cm, as shown in Fig. 9(a). Although the state feedback controllers in [32] can achieve better velocity tracking performance in the case of sensor failures, as shown in Fig. 8(b), the mean square error of the velocity is larger than the proposed controller (as shown in Table II, where we used data in [5, 10 s] when the CACC system is stable). The results indicate that the switched controller can

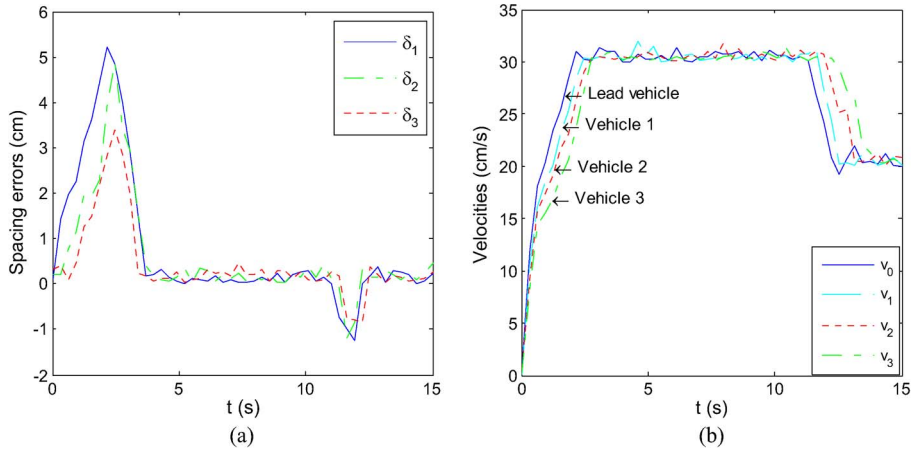

Fig. 8. Four-vehicle CACC system under switched controller. (a) Spacing errors. (b) Velocities.

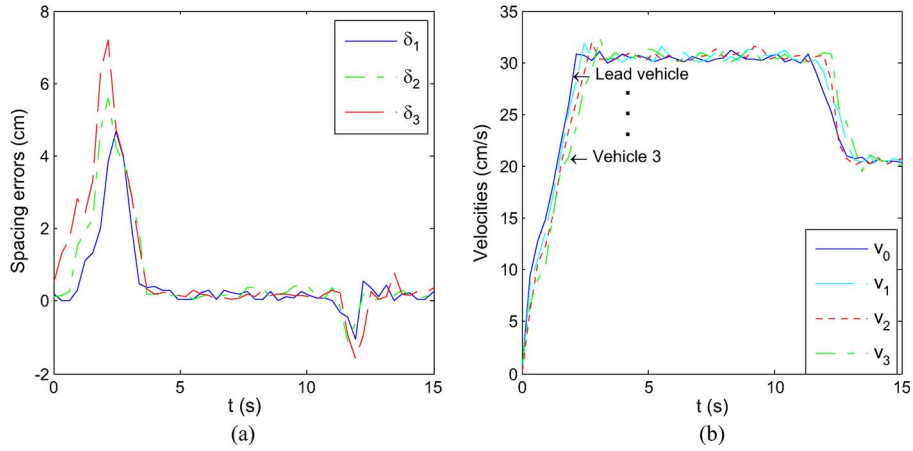

Fig. 9. Four-vehicle CACC system under controller [32]. (a) Spacing errors. (b) Velocities.

TABLE II
MEAN SQUARE VELOCITY ERRORS OF VEHICLES UNDER THE PRESENTED SWITCHING CONTROLLER AND THE CONTROLLER IN [31]

Methods	mean square velocity errors
proposed switching controller	v_1 =0.3021, v_2 =0.3135, v_3 =0.3726
controller in [31]	v_1 =0.5201, v_2 =0.5539, v_3 =0.5932

further improve the CACC system performance under the effect of sensor failures.

We also investigated the case in which there are speed bumps on the road, which was simulated by a piece of air bubble film affixed on the floor. All vehicles in the CACC system passed over the bumps one by one, as shown in Fig. 7(b) (which shows the moment when the first vehicle passed the bump). From the experimental results in Fig. 10(a) and (b) (where the maximum spacing error is 5.3 cm), we see that the speed decreases when the first vehicle passes the speed bump, and this jitter has a slight effect on the velocity of the second, third, and fourth following vehicles. Similar situations appeared when the second, the third, or the fourth vehicle passes over the bump; however, vehicle spacing is not seriously influenced [as shown in Fig. 10(a)], and the CACC system can hold string stability, showing strong robustness of the presented control method.

VI. CONCLUSION

In this paper, a sampled-date control scheme has been developed for the CACC of a string of vehicles subject to sensor failures. To reduce the negative effect of the sensor failures and communication delay, a switched control method based on the average dwell time technique was proposed. The simulation results show that the presented method is, in general, superior to existing results and that safer and smoother transient performance can be achieved by properly choosing design parameters. We further tested the results via experiments conducted with the laboratory-scale Arduino cars.

With the method presented, the controller (autonomous driver) must frequently and lightly tread the throttle and the brake pedals alternatively in order to guarantee a smooth driving performance. This may in turn imply a considerable amount of fuel (or battery) consumption in real applications. Then, a question naturally arises: How to extend the present technique to achieve a balance between string stability, driving

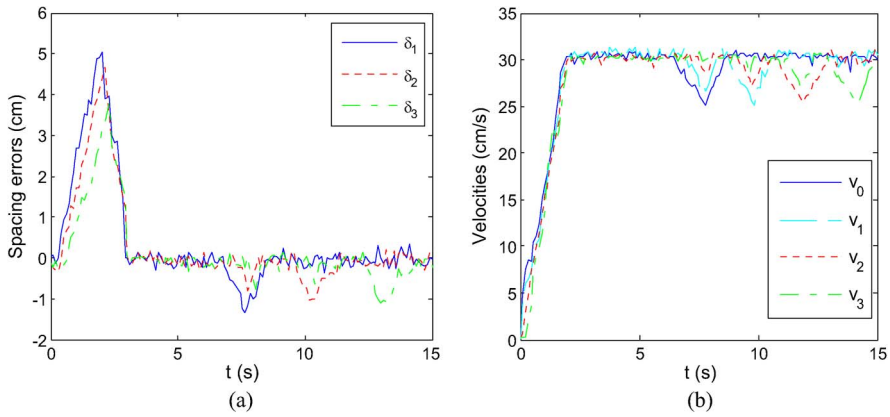

Fig. 10. Four-vehicle CACC system under switched controller. (a) Spacing errors. (b) Velocities.

performance, and energy consumption? In practical situations, vehicles may also be faced with a wide range of other challenges. For instance, the wireless communication network that the vehicles share may temporarily fail. These issues raise various open problems that are worth investigating in future research work.

APPENDIX
PROOF OF PROPOSITION 1

Here, we present the proof of Proposition 1 based on the following lemma.

Lemma 1: The following inequality:

$$\int_{t-d}^{t} \dot{x}^T(s)Q\dot{x}(s)\,ds \leq \Xi^T(t)\begin{bmatrix} M_1+M_1^T & -M_1^T+M_2 & M_3 \\ * & -M_2-M_2^T & -M_3 \\ * & * & 0 \end{bmatrix}\Xi(t) + \Xi^T(t)\begin{bmatrix} M_1^T \\ M_2^T \\ M_3^T \end{bmatrix} dQ^{-1}[M_1 \quad M_2 \quad M_3]\Xi(t) \tag{A1}$$

holds for any matrices $Q>0$, M_1, M_2, and M_3 and a scalar $d\geq 0$, where $x(t)$ and $w(t)$ are the state and disturbance variables defined in (5), i.e., $\Xi(t)=[x^T(t)\ x^T(t-d)\ w^T(t-d)]^T$.

Proof: According to the Leibniz–Newton formula, i.e.,

$$x(t)-x(t-d)-\int_{t-d}^{t}\dot{x}(s)\,ds=0. \tag{A2}$$

Hence, the following equation holds for any N_1, N_2, and $N_3\in R^{n\times n}$:

$$2\left[x^T(t)N_1^T+x^T(t-d)N_2^T+w^T(t-d)N_3^T\right]\cdot\left[x(t)-x(t-d)-\int_{t-d}^{t}\dot{x}(s)\,ds\right]=0$$

$$=2\Xi^T(t)N^T[I \quad -I \quad 0]\Xi^T(t) - 2\int_{t-d}^{t}\Xi^T(t)N^T\dot{x}(s)\,ds \tag{A3}$$

where $N=[N_1 \quad N_2 \quad N_3]$. Applying the lemma in [33] yields

$$-2\int_{t-d}^{t}\Xi^T(t)N^T\dot{x}(s)\,ds\leq\int_{t-d}^{t}\dot{x}^T(t)X\dot{x}(s)\,ds + 2\Xi^T(t)(\mathrm{Y}^T-N^T)[I \quad -I \quad 0]\Xi(t)+d\Xi^T(t)Z\Xi(t). \tag{A4}$$

Substituting (A4) into (A3) gives

$$-\int_{t-d}^{t}\Xi^T(t)N^T\dot{x}(s)\,ds \leq 2\Xi^T(t)\mathrm{Y}^T[I \quad -I \quad 0]\Xi(t)+d\Xi^T(t)Z\Xi(t) \tag{A5}$$

where $\mathrm{Y}=[M_1 \quad M_2 \quad M_3]$.

After a simple rearrangement of (A5) and applying the proposition in [33], we have (A1). This completes the proof.

Then, we give the proof of Proposition 1.

Proof: Define the following Lyapunov–Krasovskii functional for subsystem (12):

$$V_i^j(t)=x_i^T(t)P_i^jx_i(t)+2\int_{0}^{t-\tau(t)-\tau_i}w_i^T(s)C_{i2}^TR_i^jC_{i2}w_i(s)\,ds + \int_{-T}^{0}\int_{t+\theta}^{t}\dot{x}_i^T(s)e^{\alpha_i^j(s-t)}Q_i^j\dot{x}_i(s)\,ds\,d\theta \tag{A6}$$

where $j \in \{s, u\}$. Taking the derivative of V_i^j for $t \in (t_k, t_{k+1}]$ and applying Lemma 1 yield

$$\begin{aligned}\dot{V}_i^j(t) \le\ & 2x_i^T(t)P_i^j\Big[A_i x_i(t) + B_{ix}^j x_i\left(t-\tau(t)\right) \\ & + B_{iw}^j w_i\left(t-\tau(t)-\tau_i\right)\Big] \\ & + 2w_i^T\left(t-\tau(t)-\tau_i\right)C_{i2}^T R_i^j C_{i2} w_i\left(t-\tau(t)-\tau_i\right) \\ & - 2w_i^T(0)C_{i2}^T R_i^j C_{i2} w_i(0) \\ & - \alpha_i^j \int_{-T}^{0}\int_{t+\theta}^{t} \dot{x}_i^T(s)e^{\alpha_i^j(s-t)}Q_i^j\dot{x}_i(t)\,ds\,d\theta \\ & + T\dot{x}_i^T(t)Q_i^j\dot{x}_i(t) - \int_{t-T}^{t}\dot{x}_i^T(s)e^{-\alpha_i^j\varphi_i^j T}Q_i^j\dot{x}_i(s)\,ds.\end{aligned}$$

Assume that the initial condition of the preceding vehicle is steady, namely, $w_i(0) = 0$, then

$$\begin{aligned}\dot{V}_i^j(t) \le\ & -\alpha_i^j V_i^j(t) + \alpha_i^j x_i^T(t)P_i^j x_i(t) + 2x_i^T(t)P_i^j \\ & \times\Big[A_i x_i(t) + B_{ix}^j x_i\left(t-\tau(t)\right) + B_{iw}^j w_i\left(t-\tau(t)-\tau_i\right)\Big] \\ & + 2w_i^T\left(t-\tau(t)-\tau_i\right)C_{i2}^T R_i^j C_{i2} w_i\left(t-\tau(t)-\tau_i\right) \\ & + T\dot{x}_i^T(t)Q_i^j\dot{x}_i(t) - \int_{t-\tau(t)}^{t}\dot{x}_i^T(s)e^{-\alpha_i^j\varphi_i^j T}Q_i^j\dot{x}_i(s)\,ds \\ \le\ & -\alpha_i^j V_i^j(t) + \left(\eta_i(t)\right)^T\Omega_i^j\eta_i(t) \qquad \text{(A7)}\end{aligned}$$

where $\eta_i(t) = [x_i^T(t) \quad x_i^T(t-\tau(t)) \quad w_i^T(t-\tau(t)-\tau_i)]^T$. We get, by applying (13) and (A7), that $\dot{V}_i^j(t) + \alpha_i^j V_i^j(t) \le 0$, which implies

$$V_i^j(t) \le e^{-\alpha_i^j(t-t_k)}V_i^j(t_k). \qquad \text{(A8)}$$

Furthermore, since $\bigcup_{k=0}^{\infty}(t_k, t_{k+1}] = (t_0, \infty)$ and $x(t_k^+) = x(t_k)$, it follows from (A8) that (14) is true. The proof is completed.

REFERENCES

[1] A. Vahidi and A. Eskandarian, "Research advances in intelligent collision avoidance and adaptive cruise control," *IEEE Trans. Intell. Transp. Syst.*, vol. 4, no. 3, pp. 143–153, Sep. 2003.

[2] S. Li, K. Li, R. Rajamani, and J. Wang, "Model predictive multi-objective vehicular adaptive cruise control," *IEEE Trans. Control Syst. Technol.*, vol. 19, no. 3, pp. 556–566, May 2011.

[3] D. Yanakiev and I. Kanellakopoulos, "Nonlinear spacing policies for automated heavy-duty vehicles," *IEEE Trans. Veh. Technol.*, vol. 47, no. 4, pp. 1365–1377, Nov. 1998.

[4] M. R. I. Nieuwenhuijze, T. van Keulen, S. Oncu, B. Bonsen, and H. Nijmeijer, "Cooperative driving with a heavy-duty truck in mixed traffic: Experimental results," *IEEE Trans. Intell. Transp. Syst.*, vol. 13, no. 3, pp. 1026–1032, Sep. 2012.

[5] R. Rajamani and S. Shladover, "An experimental comparative study of autonomous and cooperative vehicle-follower control systems," *Transp. Res. C*, vol. 9, no. 1, pp. 15–31, Feb. 2001.

[6] C. Bonnet and H. Fritz, "Fuel reduction in a platoon: Experimental results with two electronically coupled trucks at close spacing," presented at the Future Transportation Technology Conf. Expo., Costa Mesa, CA, USA, Aug., 2000, SAE Paper 2000-01-3056.

[7] F. Browand, J. McArthur, and C. Radovich, "Fuel saving achieved in the field test of two tandem trucks," California PATH, Richmond, CA, USA, Res. Rep. UCB-ITS-PRR-2004-20, Jun. 2004.

[8] R. Rajamani and C. Y. Zhu, "Semi-autonomous adaptive cruise control systems," *IEEE Trans. Veh. Technol.*, vol. 51, no. 5, pp. 1186–1192, Sep. 2002.

[9] K. Lidstrom, K. Sjoberg, U. Holmberg, J. Andersson, and F. Bergh, "A modular CACC system integration and design," *IEEE Trans. Intell. Transp. Syst.*, vol. 13, no. 3, pp. 1050–1061, Sep. 2012.

[10] L. Guvenç *et al.*, "Cooperative adaptive cruise control implementation of Team Mekar at the Grand Cooperative Driving Challenge," *IEEE Trans. Intell. Transp. Syst.*, vol. 13, no. 3, pp. 1062–1074, Sep. 2012.

[11] G. J. L. Naus, R. P. A. Vugts, J. Ploeg, M. J. G. van de Molengraft, and M. Steinbuch, "String-stable CACC design and experimental validation: A frequency-domain approach," *IEEE Trans. Veh. Technol.*, vol. 59, no. 9, pp. 4268–4279, Nov. 2010.

[12] R. H. Middleton and J. H. Braslavsky, "String instability in classes of linear time invariant formation control with limited communication range," *IEEE Trans. Autom. Control*, vol. 55, no. 7, pp. 1519–1530, Jul. 2010.

[13] L. Xiao and F. Gao, "Practical string stability of platoon of adaptive cruise control vehicles," *IEEE Trans. Intell. Transp. Syst.*, vol. 12, no. 4, pp. 1184–1194, Dec. 2011.

[14] B. van Arem, C. van Driel, and R. Visser, "The impact of cooperative adaptive cruise control on traffic-flow characteristics," *IEEE Trans. Intell. Transp. Syst.*, vol. 7, no. 4, pp. 429–436, Dec. 2006.

[15] C. Lei *et al.*, "Impact of packet loss on CACC string stability performance," in *Proc. ITST*, 2011, pp. 381–386.

[16] C. Desjardins and B. Chaib-Draa, "Cooperative adaptive cruise control: A reinforcement learning approach," *IEEE Trans. Intell. Transp. Syst.*, vol. 12, no. 4, pp. 1248–1260, Dec. 2011.

[17] R. H. Rasshofer, M. Spies, and H. Spies, "Influences of weather phenomena on automotive laser radar systems," *Adv. Radio Sci.*, vol. 9, pp. 49–60, 2011.

[18] M. A. Fares, S. C. Fares, and C. A. Ventrice, "Attenuation of the electromagnetic waves due to moist and wet snow," in *Proc. IEEE Southeast Con*, 2007, pp. 99–104.

[19] A. A. Hassen, "Indicators for the signal degradation and optimization of automotive radar sensors under adverse weather conditions," Ph.D. dissertation, Tech. Univ. Darmstadt, Darmstadt, Germany, 2006.

[20] Z. Jia, A. Balasuriya, and S. Challa, "Sensor fusion-based visual target tracking for autonomous vehicles with the out-of-sequence measurements solution," *Robot. Autonom. Syst.*, vol. 56, no. 2, pp. 157–176, Feb. 2008.

[21] P. Caravani, E. de Santis, F. Graziosi, and E. Panizzi, "Communication control and driving assistance to a platoon of vehicles in heavy traffic and scarce visibility," *IEEE Trans. Intell. Transp. Syst.*, vol. 7, no. 4, pp. 448–460, Dec. 2006.

[22] G. Guo and W. Yue, "Autonomous platoon control allowing range-limited sensors," *IEEE Trans. Veh. Technol.*, vol. 61, no. 7, pp. 2901–2912, Sep. 2012.

[23] [Online]. Available: http://www.sharpsde.com/optoelectronics/sensors/distance-measuring-sensors/GP2D12

[24] S. Sheikholeslam and C. A. Desoer, "Longitudinal control of a platoon of vehicles with no communication of lead vehicle information," *IEEE Trans. Veh. Technol.*, vol. 42, no. 4, pp. 546–554, Nov. 1993.

[25] R. Rajesh, *Vehicle Dynamics and Control*. New York, NY, USA: Springer-Verlag, 2006.

[26] S. S. Stankovic, M. Stanojevic, and D. D. Siljak, "Decentralized suboptimal LQ control of a platoon," in *Proc. 8th IFAC/IFIP/IFORS Symp. Transp. Syst.*, 1997, vol. 1, pp. 81–86.

[27] G. H. Yang, J. L. Wang, and Y. C. Soh, "Reliable LQG control with sensor failures," *Proc. Inst. Elect. Eng.—Control Theory Appl.*, vol. 147, no. 4, pp. 433–439, Jul. 2000.

[28] E. Fridman, A. Seuret, and J. P. Richard, "Robust sampled-data stabilization of linear systems: An input delay approach," *Automatica*, vol. 40, no. 8, pp. 1441–1446, Aug. 2004.

[29] L. S. Hu, T. Bai, P. Shi, and Z. M. Wu, "Sampled-data control of networked linear control systems," *Automatica*, vol. 43, no. 5, pp. 903–911, May 2007.

[30] X. M. Zhang, M. Wu, J. H. She, and Y. He, "Delay-dependent stabilization of linear systems with time-varying state and input delays," *Automatica*, vol. 41, no. 8, pp. 1405–1412, Aug. 2005.

[31] F. W. Fu and M. van der Schaar, "Structure-aware stochastic control for transmission scheduling," *IEEE Trans. Veh. Technol.*, vol. 61, no. 9, pp. 3931–3945, Nov. 2012.

[32] S. Oncu, N. van de Wouw, and H. Nijmeijer, "Cooperative adaptive cruise control: Tradeoffs between control and network specifications," in *Proc. IEEE Intell. Transp. Syst. Conf.*, 2011, pp. 2050–2056.

[33] J. Ackerman, *Sampled Data Control Systems*. New York, NY, USA: Springer-Verlag, 1985.

Ge Guo (M'10) was born in Gansu, China, on February 23, 1972. He received the B.S. degree in automatic instrument and equipment and the Ph.D. degree in control theory and control engineering from Northeastern University, Shenyang, China, in 1994 and 1998, respectively.

In 1999 he joined Lanzhou University of Technology, Lanzhou, China, where he was the Director of the Institute of Intelligent Control and Robots and the Dean of the Department of Electric Engineering from 2000 to 2003, and also a Professor from July 2004 to May 2005. He then joined Dalian Maritime University, Dalian, China, as a Professor with the Department of Automation. From 2009 to 2010 he also held a visiting research position at The Chinese University of Hong Kong, Kowloon, Hong Kong. He is currently a Professor with the School of Control Science and Engineering, Dalian University of Technology, Dalian. He has published over 100 journal papers within his areas of interest, which include networked control systems and vehicle and mobile robot control.

Dr. Guo is the Editor-in-Chief of *International Journal of Systems, Control and Communications* and is an Associate Editor for several journals. He was an honoree of the New Century Excellent Talents in University, Ministry of Education, China, in 2004 and a nominee for Gansu Top Ten Excellent Youths by the Gansu Provincial Government in 2005.

Wei Yue was born in Shandong, China, on October 10, 1981. He received the B.S., M.E., and Ph.D. degrees in control theory and control engineering from Dalian Maritime University, Dalian, China, in 2006, 2008, and 2011, respectively.

He is a Postdoctoral Researcher with the School of Control Science and Engineering, Dalian University of Technology, Dalian. His research interests include wireless communications and intelligent vehicular platoon control.